Imprint of Accretion Disk-Induced Migration on Gravitational Waves from Extreme Mass Ratio Inspirals

Nicolás Yunes,[1,2,*] Bence Kocsis,[2] Abraham Loeb,[2] and Zoltán Haiman[3]

[1]*Department of Physics and MIT Kavli Institute, 77 Massachusetts Avenue, Cambridge, Massachusetts 02139, USA*
[2]*Harvard-Smithsonian Center for Astrophysics, 60 Garden Street, Cambridge, Massachusetts 02138, USA*
[3]*Department of Astronomy, Columbia University, 550 West 120th Street, New York, New York 10027, USA*
(Received 22 March 2011; published 21 October 2011)

We study the effects of a thin gaseous accretion disk on the inspiral of a stellar-mass black hole into a supermassive black hole. We construct a phenomenological angular momentum transport equation that reproduces known disk effects. Disk torques modify the gravitational wave phase evolution to detectable levels with LISA for reasonable disk parameters. The Fourier transform of disk-modified waveforms acquires a correction with a different frequency trend than post-Newtonian vacuum terms. Such inspirals could be used to detect accretion disks with LISA and to probe their physical parameters.

DOI: 10.1103/PhysRevLett.107.171103 PACS numbers: 04.30.Tv, 04.25.Nx, 97.10.Gz, 98.62.Mw

The inspiral of a stellar-mass compact object (CO), such as a black hole or neutron star, into a supermassive black hole (SMBH) is among the most interesting gravitational wave (GW) sources for instruments like the Laser Interferometer Space Antenna (LISA) [1]. Although LISA is currently being redesigned by the European Space Agency to accommodate a smaller budget, preliminary studies suggest that extreme mass-ratio inspirals (EMRIs) will still be detected.

EMRIs can be produced through fragmentation of accretion disks into massive stars [2,3] or through capture of compact remnants by hydrodynamic drag [4], which are believed to be mass-segregated in galactic nuclei [5], as well as through other channels [6]. Stars which reside within an accretion disk will lead to EMRIs, provided they become a CO in less time than their inward migration time. Although the expected EMRI event rate is rather uncertain (between a few tens to hundreds over LISA's lifetime, including coalescences and inspiral-only events [7]), a detectable fraction may originate in active galactic nuclei (AGNs) with an accretion disk.

Accretion disks are efficient at extracting orbital angular momentum from the extreme mass-ratio binary. The CO torques the disk gravitationally, inducing spiral density waves that carry away angular momentum [8]. In planetary disks, the same phenomenon leads to *migration* of planets towards their parent star. Planetary migration has been classified into different types (determined by disk parameters, the mass ratio, and orbital separation) to distinguish circumstances where a gap opens around the planet (Type-II) from those without a gap (Type-I). In EMRIs, migration becomes the dominant source of angular momentum transport at separations $\gtrsim 100 M_\bullet$, where $M_\bullet$ is the SMBH mass [3,9] (we use units $G = c = 1$).

Migration changes the relation between the binary's binding energy and the GW luminosity, and hence it affects the inspiral rate and the GW phase evolution. EMRIs enter the LISA sensitivity band only inside $\lesssim 50 M_\bullet$, where GW angular momentum transport is dominant. Thus, migration acts perturbatively in LISA EMRIs. In this Letter, we examine whether the imprint of migration on the EMRI GW observables is detectable by LISA. In a companion paper [10], we consider a broader range of disk effects and their impact on GWs in more detail.

Disk properties and migration.—We consider radiatively efficient, geometrically thin accretion disks, whose two most important free parameters are the accretion rate $\dot{M}_\bullet$ (overhead dots denote time derivatives) and the α-viscosity parameter. AGN observations suggest an accretion rate $\dot{M}_\bullet \equiv \dot{m}_\bullet \dot{M}_{\bullet \rm Edd} \in (0.1, 1) \dot{M}_{\bullet \rm Edd}$ [11]. Evidence for the magnitude of α is inconclusive, with plausible theoretical and observed ranges in (0.01,1) [12]. We focus on Shakura-Sunyaev α disks [13] and β disks [14], which differ in whether viscosity is proportional to the total pressure (gas plus radiation) or only the gas pressure, respectively. This affects the surface density ($\Sigma \propto r^{3/2}$ and $r^{-3/5}$ for α and β disks when opacity is dominated by electron scattering). The local disk mass is much larger for β disks at radii $r \ll 10^3 M_\bullet$, leading to a stronger GW imprint.

In the absence of a gap, Type-I migration models for angular momentum transport have been formulated [15,16] but they are very sensitive to opacity and radiation processes [17] and lack the stochastic features observed in magnetohydrodynamic simulations [18]. The presence of a gap leads to Type-II models for angular momentum exchange [19,20]. These also oversimplify the process, assuming either a steady state or quasistationarity. Type-II migration can also cease interior to a decoupling radius, r_d, in the late stages of the inspiral, when the gas accretion velocity outside the gap becomes slower than the CO's GW-driven inspiral velocity [21]. Alternatively, the gap can refill by nonaxisymmetric or 3D inflow, restoring viscous torque balance from inside and outside the CO's orbit and slowing the gaseous migration [22]. Migration is mostly unexplored in the regime relevant to LISA EMRIs, i.e., for radiation-pressure dominated, optically thick, geometrically thin, relativistic, magnetized and turbulent disks, with the CO's mass $m_\star$ exceeding the local disk mass.

Astrophysical uncertainties regarding accretion disks and migration in the regime relevant to LISA EMRIs lead us to consider a general power-law relation,

$$\dot{\ell}_\star = \dot{\ell}_{\rm GW}(1 + \delta\dot{\ell}), \tag{1}$$

$$\delta\dot{\ell} \equiv A\bar{r}^B = A_0 \alpha_1^{A_1} \dot{m}_{\bullet 1}^{A_2} M_{\bullet 5}^{A_3} m_{\star 1}^{A_4} \bar{r}^B, \tag{2}$$

where $\dot{\ell}_\star$ is the CO's rate of change of specific angular momentum, $\dot{\ell}_{\rm GW}$ is the loss due to GWs [10], and $\delta\dot{\ell}$ a correction induced by migration. The power-law form in the reduced radius $\bar{r} \equiv r/M_\bullet$ involves an amplitude A, which is parameterized in terms of normalized accretion disk ($\alpha_1 \equiv \alpha/0.1$, $\dot{m}_{\bullet 1} = \dot{m}_\bullet/0.1$), and mass parameters [$M_{\bullet 5} = M_\bullet/(10^5 M_\odot)$, $m_{\star 1} = m_\star/(10 M_\odot)$]. The power-law indices ($A_{i>0}$, B) are given in Table I for representative migration models: rows 1–2 correspond to Type-I [16], 3–4 to steady state Type-II [19], 5 to quasistationary Type-II migration in the asymptotic limit for small $\bar{r}$ [20] (the latter is available for β disks only). The gap decouples and Type-II migration ceases ($A \approx 0$) interior to $\bar{r}_d = 1.4 \times 10^{-5} \alpha_1^{-2} \dot{m}_{\bullet 1}^{-4} M_{\bullet 5}^{-2} m_{\star 1}^2 \lambda^5$ for α and $15 \alpha_1^{-4/13} \dot{m}_{\bullet 1}^{-2/13} M_{\bullet 5}^{-4/13} m_{\star 1}^{5/13} \lambda^{2/13}$ for β disks, where (λr) is the gap radius (we adopt $\lambda = 1.7$ [23]). Since disk effects become stronger at larger radii, $B > 0$.

GW implications.—The change in the angular momentum dissipation rate due to migration modifies the GW evolution, leading to a change in the accumulated GW phase and spectrum. For circular orbits, the quadrupolar GW phase can be computed from $\phi_{\rm GW} = 2\int_{r_0'}^{r_f} dr \Omega \dot{\ell}_\star^{-1} d\ell/dr$, where the orbital frequency is $\Omega \simeq (M_\bullet/r^3)^{1/2}$, the binary's specific angular momentum is $\ell = r^2\Omega = M_\bullet^{1/2} r^{1/2}$, while the specific angular momentum flux $\dot{\ell}_\star$ is given by Eq. (1). For a fixed final EMRI separation r_f and observation time $T_{\rm obs}$, the initial separation r_0' is different from r_0 (the initial separation in vacuum), as the radial inspiral evolution $\dot{r}$ is determined by $\dot{\ell}_\star$: $r = \int_{r_0'}^{r_f} \dot{\ell}_\star (d\ell/dr)^{-1} dr$. For an unperturbed EMRI, $(\bar{r}_f/\bar{r}_0)^{-4} \approx 1 + 33(m_{\star 1}/M_{\bullet 5}^2)(T_{\rm obs}/{\rm yr})(\bar{r}_f/10)^{-4}$.

The correction to the GW phase given the same observation time for perturbed and unperturbed orbits, $\delta\phi_{\rm GW} \equiv \phi_{\rm GW} - \phi_{\rm GW}^{\rm vac}$, where $\phi_{\rm GW}^{\rm vac}$ is the accumulated phase in vacuum, is then

$$\delta\phi_{\rm GW} = \bar{A} \frac{M_{\bullet 5}}{m_{\star 1}} \bar{r}_0^{B+5/2} \times \left(1 + \frac{2B+5}{3} x^{B+4} - \frac{2B+8}{3} x^{B+5/2}\right), \tag{3}$$

where $\bar{A} \equiv -(3 \times 4^{-1/2} \times 5^5)(4+B)^{-1}(5+2B)^{-1} A$, $x \equiv r_f/r_0$, $\bar{r}_0 \equiv r_0/M_\bullet$ and we have expanded in $\delta\dot{\ell} \ll 1$, which holds in the LISA regime. For fixed $T_{\rm obs}$, we find that $|\delta\phi_{\rm GW}|$ increases and decreases with $m_\star$ for the Type-I and II models of Table I, respectively.

The top panel of Fig. 1 plots the dephasing in Eq. (3) for two typical LISA EMRIs at fixed $r_f > r_d$ as contours for different torque parameters (A, B). The specific migration models defined in Table I with $\alpha_1 = 1 = \dot{m}_{\bullet 1}$ are marked with symbols. The bottom panel shows $\delta\phi_{\rm GW}$ for those models but with different r_f, fixing $T_{\rm obs} = 1$ yr (cf. LISA's planned lifetime is 3 years). For comparison, we also plot the total GW phase accumulation [$\mathcal{O}(10^6)$ top, thin line] and a rough measure of LISA's accuracy to phase measurements: $\delta\phi_{\rm GW} > 10/\rho$, where ρ is the signal-to-noise ratio $\rho(h) = 4\int_{r_0}^{r_f} dr (df/dr) |\tilde{h}|^2 S_n^{-1}[f(r)]$, with $S_n[f(r)]$ the LISA detector noise [24] and $\tilde{h}$ the Fourier transform of the orientation-averaged GW signal. We evaluate ρ at 1 Gpc (or redshift $z \approx 0.2$; thick solid line) and at 10 Mpc (or $z \approx 0.002$; thick dashed line). For $\rho < 10$, we assume the EMRI is not detected at all, which explains the sharp rise in the detection level beyond a certain r_f. Migration with a gap (empty symbols) causes a bigger phase shift because of the pileup of mass outside the gap. For $\bar{r}_d \lesssim \bar{r}_f \lesssim 50$ but fixed (A, B, $M_\bullet$, $m_\star$, $T_{\rm obs}$), the phase shift is constant within a factor $\sim$3, but it quickly drops off for the Type-II models interior to the gap decoupling radius r_d where $A \to 0$.

The Newtonian estimates presented here suggest that LISA EMRI observations might be able to probe accretion-disk-induced migration. Figure 1 shows that a large sector of parameter space (A, B) exists where the dephasing is large enough to be detectable, and $\delta\phi_{\rm GW}$ is very sensitive to the disk model and its parameters. One might worry, however, that the estimates in Fig. 1 are inaccurate due to the use of a Newtonian waveform model. We have verified that this is not the case through a relativistic

TABLE I. Disk parameters for Type-I and II migration models in α and β disks.

		A_0	A_1	A_2	A_3	A_4	B
[16], Iα	●	7.2×10^{-19}	-1	-3	1	0	8
[16], Iβ	●	6.5×10^{-13}	$-4/5$	$-7/5$	6/5	0	59/10
[19], IIα	□	6.2×10^{-10}	0	1	3	-2	4
[19], IIβ	□	4.4×10^{-6}	1/2	5/8	13/8	$-11/8$	25/8
[20], IIβ	△	1.6×10^{-7}	2/7	11/14	31/14	$-23/14$	7/2

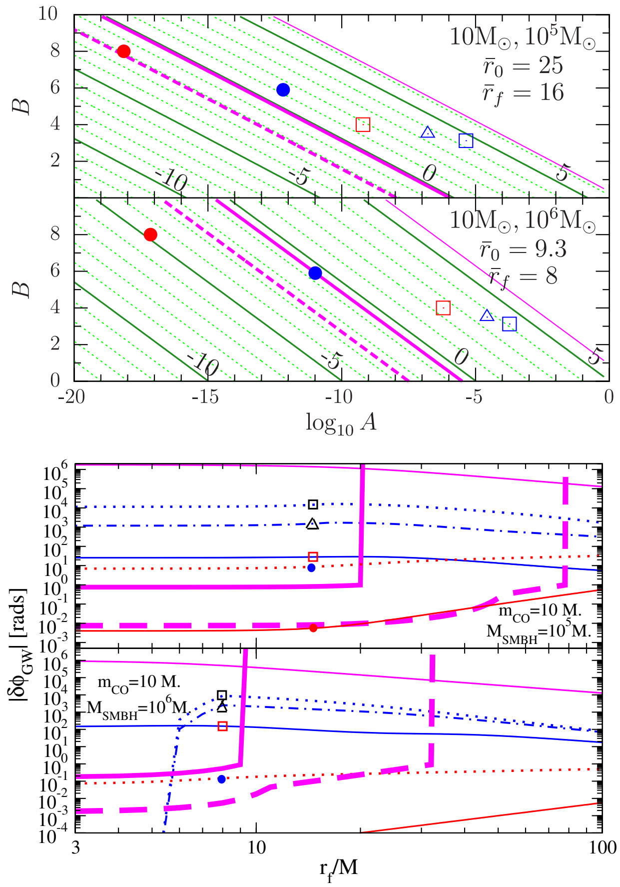

FIG. 1 (color online). Top: contours of $\log_{10}|\delta\phi_{\rm GW}|$ for different interaction models of two EMRI systems observed for 1 yr. The symbols represent the models in Table I. Bottom: $|\delta\phi_{\rm GW}|$ versus $\bar{r}_f$ for the 5 models in Table I [Type-I, α (β) in solid (dotted) red, Type-II α in solid blue, Type-II β of [19,20] in dotted and dot-dashed blue, respectively]. The symbols represent the EMRIs considered in [10]. Many of the models—especially those resembling β disks and Type-II migration—shown in Table I lie well above the LISA sensitivity level [thick solid (optimistic) and dashed (pessimistic) magenta lines].

waveform model that employs the calibrated effective-one-body scheme [25]. We have generated 1 yr-long waveforms for the systems plotted in Fig. 1 and included modifications to the radiation-reaction force due to migration, as parameterized by Eq. (2). Overall, we find the Newtonian results to be representative of the fully relativistic ones [10].

Just because migration produces a sufficiently large phase correction does not necessarily imply that LISA can measure it. For that to be possible, migration phase corrections must be nondegenerate, or at worst, weakly correlated with other system parameters. One can study if this is the case by computing the Fourier transform of the GW observable. We employ the stationary phase approximation (SPA) [26], where one assumes the GW phase varies much more rapidly than the amplitude. The Fourier transform of $h(t) = A(t)\exp[i\phi_{\rm GW}(t)]$ can then be approximated as $\tilde{h}(f) = \tilde{A}(f)\exp[i\psi(f)]$, where $\tilde{A}(f) \equiv (4/5)A[t(f)]\dot{f}^{-1/2}$ and $\psi(f) \equiv 2\pi f t_0 - \phi_{\rm GW}(t_0)$, where f is the GW frequency and t_0 is the stationary point, defined by $2\pi f = (d\phi_{\rm GW}/dt)_{t=t_0}$ [26].

The corrections due to migration on the Fourier transform of the GW phase in the SPA, $\delta\psi \equiv \psi - \psi_{\rm vac}$, are

$$\frac{\delta\psi}{\psi_{\rm vac}^{\rm Newt}} = \tilde{A}\bar{\eta}^{2B/5}\bar{u}^{-2B/3}, \tag{4}$$

where we have defined $\tilde{A} \equiv -2^{2-8B/5}5^{1-8B/5}(4+B)^{-1}\times(5+2B)^{-1}A\exp(6.46B)$, the normalized symmetric mass ratio $\bar{\eta} \equiv m_{\star 1}/M_{\bullet 5}$ and $\bar{u} \equiv (\pi\mathcal{M}f)/(6.15\times 10^{-5})$, and where $\mathcal{M} = m_\star^{3/5}M_\bullet^{2/5}$ is the chirp mass and $\psi_{\rm vac}^{\rm Newt} = (3/128)(\pi\mathcal{M}f)^{-5/3}$ is the leading-order (Newtonian) vacuum Fourier phase. The amplitude of the SPA Fourier transform is corrected in a similar fashion $\delta|\tilde{h}|/|\tilde{h}|_{\rm vac}^{\rm Newt} \sim \delta\psi/\psi_{\rm vac}^{\rm Newt}$.

Equation (4) is to be compared with the intrinsic general relativity (GR) corrections to the vacuum Fourier GW phase: $\psi_{\rm vac}/\psi_{\rm vac}^{\rm Newt} = \sum_{n=0}^{\infty} a_n u^{2n/3}$, where $a_q = a_q(m_\star, M_\bullet)$, and the modulation induced by the orbital motion of LISA around the Sun. Migration corrections lead to negative frequency exponents in the Fourier phase (in Eq. (4), $-2B/3 < 0$), while GR, post-Newtonian corrections in vacuum lead to positive powers of frequency, while the detector orbit is periodic with a 1 yr period. For a sufficiently strong signal, this suggests it might be possible to separate the migration effects from the other GR and detector orbit induced phase corrections.

Modified gravity theories might introduce corrections similar to Eq. (4). The parameterized post-Einsteinian (ppE) framework [27], devised to search for generic GR deviations in GW data, postulated such a phase modification, allowing for both positive and negative B. Degeneracies between disk and modified gravity effects with negative frequency exponents ($B > 0$) could then exist (e.g., Brans-Dicke theory or $G(t)$ theories). The latter, however, have already been greatly constrained by binary pulsar observations [28]. Moreover, alternative theory modifications should be present in all EMRIs, while disk effects will be present in only a small subset.

A precise measure of whether a migration-modified waveform $\tilde{h}_1(f)$ is distinguishable from a vacuum waveform $\tilde{h}_2(f;\vec{\lambda})$, where $\vec{\lambda}$ stands for all disk parameters, requires a detailed Monte Carlo study that maps the likelihood surface. A rough measure of distinguishability can be obtained by calculating the signal-to-noise ratio (SNR) of the difference between a vacuum and a nonvacuum waveform $\rho(\delta h)$ by minimizing only over a time and a phase shift. Using this crude measure, we demonstrate in the bottom panel of Fig. 2 that most of the migration models of Table I lead to $\rho(\delta h) > 10$ within 5 months of observation for a source at 1 Gpc.

Going beyond Table I, there exists a large sector of disk parameter space (A, B) for which the SNR of the waveform

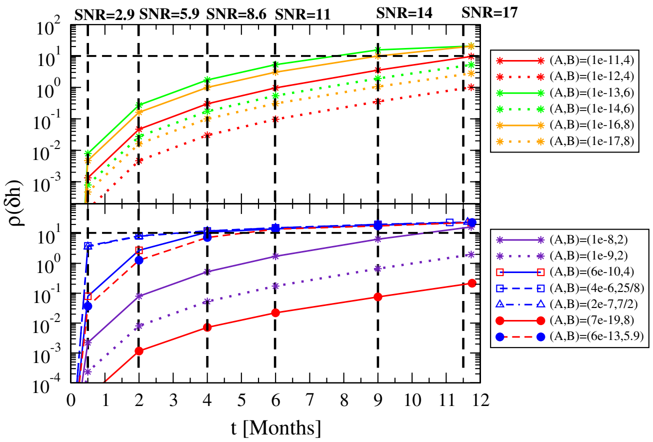

FIG. 2 (color online). $\rho(\delta h)$ as a function of observation time. Observe that $\rho(\delta h) > 5$ within 1 yr for a large set of (A, B).

difference exceeds threshold $\rho(\delta h) > 10$. Figure 2 plots $\rho(\delta h)$ at 1 Gpc as a function of observation time for different values of (A, B) in Eq. (2). We also indicate (with labels over the vertical dashed lines) the SNR of the vacuum waveform at 1 Gpc and $T = (0.5, 2, 4, 6, 9, 11.5)$ months. We calculate the waveforms with the relativistic model of [25] and $(M_{\bullet 5}, m_{\star 1}) = (1, 1)$, SMBH spin angular momentum $|S_\bullet| = 0.9 M_\bullet^2$ coaligned with the orbital angular momentum, and initial and final separations $(r_0, r_f) \sim (24.5, 16) M_\bullet$. Observe that for a large set of disk parameters (A, B), $\rho(\delta h) > 10$ within a one-year observation. Fitting to the smallest A with $\rho(\delta h) > 10$ for fixed B, we find that for these masses and orbital radii, LISA could measure $\log_{10} A \gtrsim a_1 + a_2 B$, with $a_1 = -5.7 \pm 0.4$ and $a_2 = -1.4 \pm 0.2$.

Discussion.—The GW observation of EMRI signals with LISA could be used to probe the uncertain physics of accretion disks. In particular, spiral density waves generated by an orbiting CO can transfer sufficient orbital angular momentum to alter the GW signal at levels that are detectable by LISA. Although the effect is negligible for Type-I migration in α disks as found by Levin [3], we find it to be significant for parameter choices resembling Type-II migration (i.e. with the CO opening a gap) or for β disk models. A very crude (diagonal) Fisher analysis suggests that LISA could measure certain sectors of disk parameter space to better than 10%, for vacuum SNRs larger than 10 [10]. This is no surprise considering that $\delta\phi_{\rm GW}$ is at worst $\sim$10 times higher than LISA's sensitive curve in Fig. 1. Detection of the predicted migration effect would reduce the uncertainty in existing theoretical models and offer the potential for extending the discussion to more complicated geometries (such as EMRIs with eccentric and/or inclined orbits).

The detection of EMRIs in AGNs and the extraction of disk parameters improve the prospects for finding electromagnetic counterparts in the LISA error volume with consistent luminosities [29]. Coincident measurements would also allow EMRIs to serve as standard sirens to independently test cosmological models [30]. LISA EMRIs are low-redshift events, for which weak lensing errors, dominant in comparable mass, SMBH standard sirens at higher-z, are subdominant [29]. Disk effects will not compromise the ability to constrain cosmological parameters, as they enter the GW observable with a different frequency signature, and are thus weakly correlated. Migration effects may also deplete the unresolved low-frequency EMRIs that contribute to the GW confusion noise background [24].

B. K. and N. Y. acknowledge support from the NASA through Einstein Fellowship PF9-00063 and PF0-110080 issued by the Chandra X-ray Observatory, operated by the SAO, on behalf of NASA under NAS8-03060. A. L. acknowledges support from NSF grant AST-0907890 and NASA grants NNX08AL43G and NNA09DB30A, Z. H. from the Polányi Program of the Hungarian National Office for Research and Technology (NKTH) and from NASA grant NNX08AH35G, and B. K. from the Hungarian Research Fund (OTKA) grant 68228.

*Present address: Department of Physics, Montana State University, Bozeman, MT 59717, USA.

[1] LISA, www.esa.int/science/lisa.
[2] J. Goodman and J. C. Tan, Astrophys. J. **608**, 108 (2004).
[3] Y. Levin, Mon. Not. R. Astron. Soc. **374**, 515 (2007).
[4] L. Šubr and V. Karas, Astron. Astrophys. **352**, 452 (1999); J. MiraldaEscudé and J. A. Kollmeier, Astrophys. J. **619**, 30 (2005).
[5] M. Freitag, P. Amaro-Seoane, and V. Kalogera, Astrophys. J. **649**, 91 (2006).
[6] P. Amaro-Seoane, J. R. Gair, M. Freitag, M. C. Miller, I. Mandel, C. J. Cutler, and S. Babak, Classical Quantum Gravity **24**, R113 (2007).
[7] J. R. Gair, Classical Quantum Gravity **26**, 094034 (2009).
[8] W. R. Ward, Icarus **126**, 261 (1997).
[9] V. Karas and L. Šubr, Astron. Astrophys. **376**, 686 (2001).
[10] B. Kocsis, N. Yunes, and A. Loeb, Phys. Rev. D **84**, 024032 (2011).
[11] J. A. Kollmeier *et al.*, Astrophys. J. **648**, 128 (2006).
[12] A. R. King, J. E. Pringle, and M. Livio, Mon. Not. R. Astron. Soc. **376**, 1740 (2007).
[13] N. I. Shakura and R. A. Sunyaev, Astron. Astrophys. **24**, 337 (1973).
[14] P. J. Sakimoto and F. V. Coroniti, Astrophys. J. **247**, 19 (1981).
[15] P. Goldreich and S. Tremaine, Astrophys. J. **241**, 425 (1980).
[16] H. Tanaka, T. Takeuchi, and W. R. Ward, Astrophys. J. **565**, 1257 (2002).
[17] S. Paardekooper and G. Mellema, Astron. Astrophys. **459**, L17 (2006).
[18] R. P. Nelson and J. C. B. Papaloizou, Mon. Not. R. Astron. Soc. **350**, 849 (2004); G. Laughlin, A. Steinacker, and F. C. Adams, Astrophys. J. **608**, 489 (2004).

[19] D. Syer and C. J. Clarke, Mon. Not. R. Astron. Soc. **277**, 758 (1995).
[20] P. B. Ivanov, J. C. B. Papaloizou, and A. G. Polnarev, Mon. Not. R. Astron. Soc. **307**, 79 (1999).
[21] M. Milosavljević and E. S. Phinney, Astrophys. J. **622**, L93 (2005); Z. Haiman, B. Kocsis, and K. Menou, Astrophys. J. **700**, 1952 (2009).
[22] P. Artymowicz and S. H. Lubow, Astrophys. J. **467**, L77 (1996); A. I. MacFadyen and M. Milosavljević, Astrophys. J. **672**, 83 (2008); J. Cuadra, P. J. Armitage, R. D. Alexander, and M. C. Begelman, Mon. Not. R. Astron. Soc. **393**, 1423 (2009).
[23] P. Artymowicz and S. H. Lubow, Astrophys. J. **421**, 651 (1994).
[24] L. Barack and C. Cutler, Phys. Rev. D **70**, 122002 (2004).
[25] N. Yunes, A. Buonanno, S. A. Hughes, M. C. Miller, and Y. Pan, Phys. Rev. Lett. **104**, 091102 (2010); N. Yunes, GW Notes **2**, 3 (2009); N. Yunes *et al.* (2010).
[26] E. Poisson and C. M. Will, Phys. Rev. D **52**, 848 (1995); N. Yunes, K. Arun, E. Berti, and C. M. Will, Phys. Rev. D **80**, 084001 (2009).
[27] N. Yunes and F. Pretorius, Phys. Rev. D **80**, 122003 (2009).
[28] N. Yunes, F. Pretorius, and D. Spergel, Phys. Rev. D **81**, 064018 (2010).
[29] B. Kocsis, Z. Frei, Z. Haiman, and K. Menou, Astrophys. J. **637**, 27 (2006); B. Kocsis, Z. Haiman, and K. Menou, Astrophys. J. **684**, 870 (2008).
[30] B. F. Schutz, Nature (London) **323**, 310 (1986); D. E. Holz and S. A. Hughes, Astrophys. J. **629**, 15 (2005).